

Chemical Reaction on Heat and Mass Flow Past a Vertical Cylinder Embedded in Non-Darcy Porous Medium

B. Vasu^{1,*}, Rama S R Gorla², V. R. Prasad³ and O. A. Beg⁴

¹Department of Mathematics, Motilal Nehru National Institute of Technology, Allahabad - 211004, India

²Department of Mechanical & Civil Engineering, Purdue University Northwest, Westville, Indiana 46391, USA

³Department of Mathematics, Madanapalle Institute of Technology and Science, Madanapalle-517325, India

⁴Department of Mechanical and Aeronautical Engineering, School of Computing, Science and Engineering, Newton Building, Salford University, Salford, M54WT, UK

Abstract

An unsteady two-dimensional free convection flow of a viscous incompressible fluid past an impulsively started semi-infinite vertical cylinder adjacent to a non-Darcian porous media in the presence of chemical reaction of first order is investigated. The governing boundary layer equations are formulated with appropriate boundary conditions and are solved using an implicit finite-difference method of Crank-Nicholson type. The problem is shown to be controlled by seven thermophysical and hydrodynamic dimensionless parameters, namely thermal Grashof number (Gr), species Grashof number (Gm), Darcy number (Da i.e. permeability parameter), Forchheimer number (Fs i.e. second order inertial porous parameter), Prandtl number (Pr), Schmidt number (Sc) and chemical reaction parameter (K_1). The effects of thermophysical parameter on the transient dimensionless velocity, temperature and concentration are illustrated graphically. Also, the effects of the various thermo-physical parameters on the Skin friction, Nusselt number and Sherwood number are presented and discussed. This model finds applications in polymer production, manufacturing of ceramics or glassware and food processing.

Keywords: *Transient thermal convection; chemical reaction; Forchheimer number; Nusselt number; Sherwood number; vertical cylinder.*

Nomenclature

C'	species concentration	t	time
C	dimensionless concentration	τ'	temperature
Da	Darcy number	τ	dimensionless temperature
Fs	Forchheimer number	T_∞, C_∞	free stream temperature, concentration
g	gravitational acceleration	X	dimensionless axial coordinate
Gr	thermal Grashof number	x	axial coordinate measured vertically upward
Gm	species Grashof number	U, V	dimensionless velocity components along the X- and R-directions
K	permeability of porous medium	u, v	velocity components along the x, r directions
k	thermal conductivity of fluid	Nu_x	dimensionless local Nusselt number
K_1	chemical reaction parameter	\overline{Nu}	average Nusselt number
Pr	Prandtl number	Sh_x	dimensionless local Sherwood number
R	dimensionless radial coordinate	\overline{Sh}	average Sherwood number
r	radial coordinate		
Sc	Schmidt number		

Greek symbols

α	thermal diffusivity	β^*	volumetric coefficient of expansion with concentration
β	volumetric thermal expansion coefficient	τ_x	dimensionless local shear stress function (skin friction)
μ	dynamic viscosity of fluid		
ν	kinematic viscosity of fluid		

1. Introduction

Unsteady free convection flow of a viscous incompressible fluid along a vertical or horizontal heated cylinder is an important problem relevant to many engineering applications such as geothermal power generation and drilling operations, where the free-stream and buoyancy induced fluid velocities are of roughly the same order of magnitude. The exact solution for these types of non-linear problems is still out of reach. Sparrow and Gregg [1] provided the first approximate solution for the laminar buoyant flow of air bathing a vertical cylinder heated with a prescribed surface temperature, by applying the similarity method and power series expansion. Minkowycz and Sparrow [2] obtained the solution for the same problem using the non-similarity method. Fujii and Uehara [3] analyzed the local heat transfer results for arbitrary Prandtl numbers. Lee et al. [4] investigated the problem of natural convection in laminar boundary layer flow along slender vertical cylinders and needles for the power-law variation in wall temperature. Rani [5] has investigated the unsteady natural convection flow over a vertical cylinder with variable heat and mass transfer using the finite difference method. Ganesan and Loganathan [6] solved the problem of unsteady natural convective flow past a moving vertical cylinder with heat and mass transfer.

Chemical reactions can be codified as either heterogeneous or homogeneous processes. This depends on whether they occur at an interface or as a single phase volume reaction. In many chemical engineering processes, there does occur the chemical reaction between a foreign mass and the fluid in which the cylinder is moving. These processes take place in numerous industrial applications, e.g., polymer production, manufacturing of ceramics or glassware and food processing. Mass transfer effects on moving isothermal vertical plate in the presence of chemical reaction studied by Das et al [7]. The dimensionless governing equations were solved by the usual Laplace transform technique and the solutions are valid only at lower time level. Ghaly and Seddeek [8] presented Chebyshev finite difference solution for viscosity effects on the chemically-reacting heat and mass transfer along a semi-infinite horizontal plate. Muthucumaraswamy and Ganesan [9] presented finite-difference solutions for the effect of first-order chemical reaction on flow past an impulsively started vertical plate with uniform heat and mass flux, showing that chemical reaction parameter reduces velocities. Ganesan and Loganathan [10] investigated the chemically reactive heat and mass transfer in boundary layer convection from a moving vertical cylinder.

Computational transport modelling of buoyancy flows in geomaterials is of considerable interest in environmental and civil engineering sciences. Environmental transport processes in soils, forest fire development through brush and dry soils, geothermal processes, radioactive waste storage and thermal plumes in magmatic geo-systems constitute just a few important applications of geological thermofluid transport modelling. A thorough discussion of these and other applications is available in the monographs by Ingham and Pop [11] and Nield and Bejan [12]. The vast majority of porous media transport models have employed the Darcian model which for isotropic, homogenous materials utilizes a single permeability for simulating the global effects of the porous medium on the flow. Effectively in the context of viscous hydrodynamic modelling, for example using boundary-layer theory, the momentum conservation equation (unidirectional Navier–Stokes

equation) is supplemented by an additional body force, the Darcian bulk linear drag. Numerous studies in the context of transport modelling in soil mechanics, petroleum displacement in reservoirs, geothermics, geo-hydrology and filtration physics have employed such an approach. For example, Singh et al. [13] studied the free convection flow and heat transfer in a Darcian porous geo-material using perturbation methods; this study also incorporated permeability variation via a transverse periodic function. Thomas and Li [14] analyzed numerically the unsteady coupled heat and mass transfer in unsaturated soil with a Darcy model. The Darcy model assumes that the pressure drop across the geo-material is proportional to the bulk drag force. At higher velocities, however, inertial effects become important and the regime is no longer viscous dominated. The most popular approach for simulating high-velocity transport in porous media, which may occur for example under strong buoyancy forces, through highly porous materials, etc., is the Darcy–Forchheimer drag force model. This adds a second-order (quadratic) drag force to the momentum transport equation. This term is related to the geometrical features of the porous medium and is independent of viscosity, as has been shown rigorously by Dybbs and Edwards [15]. In the context of coupled heat and mass transfer studies, Kumari et al. [16] studied the double diffusive heat and species transport in porous media using the Darcy–Forchheimer model. Takhar and Bég [17] used the Keller–Box implicit difference method to analyze the viscosity and thermal conductivity effects in boundary layer thermal convection in non-Darcian porous media. Beg et al. [18] studied using NSM the unsteady hydrodynamic couette flow through a rotating porous medium channel using a Forchheimer-extended Darcy model. Vallampati et al. [19] presented a numerical solution for the free convective, unsteady, laminar convective heat and mass transfer in a viscoelastic fluid along a semi-infinite vertical plate. Radiation and mass transfer effects on two-dimensional flow past an impulsively started isothermal vertical plate were analyzed by Prasad et al. [20]. Cooney et al [21] investigated the problem of MHD free convection and oscillating flow of an optically thin fluid bounded by two horizontal porous parallel walls with a periodic wall temperature. Chuo-Jeng Huang [22] numerically analyzed the heat and mass transfer characteristics of natural convection about a vertical flat plate embedded in a saturated porous medium with blowing/suction and thermal radiation effects considering Soret and Dufour. Sharma and Dutt [23] studied the effect of magnetic field on unsteady free convection oscillatory flow through vertical porous plate, when free stream velocity, wall temperature and concentration are periodic. The unsteady mixed convective fluid flow through an annulus filled with a fluid saturated porous medium in the presence of cross-diffusion effect and constant heat source is numerically investigated by Muli and Kwanza [24].

This work however only considered the vertical cylinder scenario. Clearly much remains to be explored in this topic, both in the way of geometrical bodies in the porous media (e.g. cones, spheres, ellipsoids, wedges, cylinders) and also regarding interactive effects of the thermophysical parameters. The objective of the present work is therefore to investigate the free convection simultaneous heat and mass transfer flow from a vertical cylinder embedded in fluid saturated porous medium with Darcian resistance, Forchheimer quadratic drag, chemical reaction, thermal Grashof number, species Grashof number, Prandtl number and Schmidt number effects. The effects of governing multi-physical parameters on heat and mass transfer characteristics are analyzed. The non-linear coupled partial differential equations governing the flow field have been solved numerically by using an implicit finite difference method of Crank – Nicolson type. These processes take place in numerous industrial applications, e.g., polymer production, manufacturing of ceramics or glassware and food processing.

The behavior of the velocity, temperature, concentration, skin friction, Nusselt and Sherwood numbers have been discoursed for variations in governing parameters, and benchmarked where appropriate with previous studies.

2. Mathematical Analysis

Consider a two-dimensional unsteady free convection heat and mass transfer flow from a vertical cylinder of radius r_0 embedded in an isotropic, homogenous, fully-saturated porous medium as shown in Figure 1. The x -axis is measured vertically upward along the axis of the cylinder. The origin of x is taken to be at the leading edge of the cylinder, where the boundary layer thickness is zero. The radial coordinate r is measured perpendicular to the axis of the cylinder. The surrounding stationary fluid temperature is assumed to be of ambient temperature (T'_∞). Initially, i.e., at $t' = 0$ it is assumed that the cylinder and the fluid are of the same temperature T'_∞ . When $t' > 0$, the temperature of the cylinder is raised to $T'_w > T'_\infty$ and maintained at the same level for all the time $t' > 0$.

To derive the basic equations for the problem under consideration, the following assumptions are made:

- (i) The flow is unsteady and free convection embedded in porous medium.
- (ii) The fluid under consideration is viscous incompressible and electrically conducting with constant physical properties.
- (iii) The magnetic Reynolds number is assumed to be small enough so that the induced magnetic field can be neglected.
- (iv) The effect of the viscous dissipation and Joule heating are assumed to be negligible in the energy equation.
- (v) There is a homogeneous chemical reaction of first order with rate constant K_1 between the diffusing species and the fluid.
- (vi) Also, the mass diffusion and heat diffusion are assumed to be independent on each other.

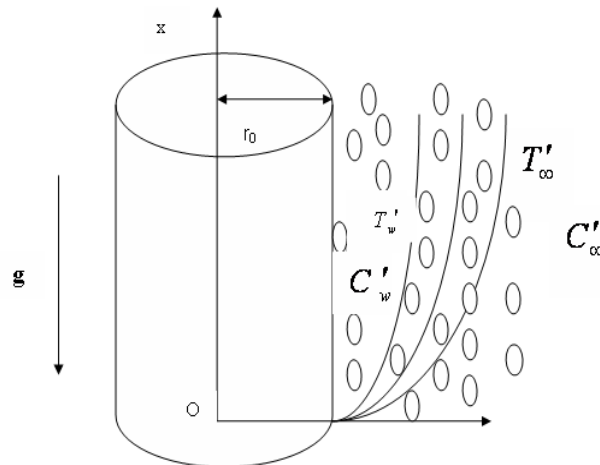


Figure 1. Physical model and Coordinate system

Under these assumptions, the boundary layer equations of mass, momentum and energy with Boussinesq's approximation are as follows:

Continuity equation

$$\frac{\partial(ru)}{\partial x} + \frac{\partial(rv)}{\partial r} = 0 \quad (1)$$

Momentum equation

$$\frac{\partial u}{\partial t'} + u \frac{\partial u}{\partial x} + v \frac{\partial u}{\partial r} = g\beta(T' - T'_\infty) + g\beta^*(C' - C'_\infty) + \frac{\nu}{r} \frac{\partial}{\partial r} \left(r \frac{\partial u}{\partial r} \right) - \frac{\nu}{K} u - \frac{b}{K} u^2 \quad (2)$$

Energy equation

$$\frac{\partial T'}{\partial t'} + u \frac{\partial T'}{\partial x} + v \frac{\partial T'}{\partial r} = \frac{k}{\rho c_p} \frac{1}{r} \frac{\partial}{\partial r} \left(r \frac{\partial T'}{\partial r} \right) \quad (3)$$

Mass diffusion equation

$$\frac{\partial C'}{\partial t'} + u \frac{\partial C'}{\partial x} + v \frac{\partial C'}{\partial r} = \frac{D}{r} \frac{\partial}{\partial r} \left(r \frac{\partial C'}{\partial r} \right) - K_l C' \quad (4)$$

The initial and boundary conditions are:

$$\begin{aligned} t' \leq 0: \quad u = 0, \quad v = 0, \quad T' = T'_\infty, \quad C' = C'_\infty & \quad \text{for all } x \geq 0 \text{ and } r \geq 0 \\ t' > 0: \quad u = u_0, \quad v = 0, \quad T' = T'_w, \quad C' = C'_w & \quad \text{at } r = r_0 \\ u = 0, \quad v = 0, \quad T' = T'_\infty, \quad C' = C'_\infty & \quad \text{at } x = 0 \text{ and } r > r_0 \\ u \rightarrow 0, \quad T' \rightarrow T'_\infty, \quad C' \rightarrow C'_\infty & \quad \text{as } r \rightarrow \infty \end{aligned} \quad (5)$$

where u, v are the velocity components in x, r directions respectively, t' - the time, g - the acceleration due to gravity, β - the volumetric coefficient of thermal expansion, β^* - the volumetric coefficient of expansion with concentration, T' - the temperature of the fluid in the boundary layer, C' - the species concentration in the boundary layer, T'_w - the wall temperature, C'_w - the concentration at the wall, T'_∞ - the free stream temperature of the fluid far away from the plate, C'_∞ - the species concentration in fluid far away from the cylinder, ν - the kinematic viscosity, ρ - the density of the fluid, c_p - the specific heat at constant pressure, k - permeability, b - Forchheimer geometrical inertial parameter for the porous medium K_l - Chemical reaction rate and D - the species diffusion coefficient. In the momentum equation (2) the first two terms on the right-hand side represent the thermal buoyancy body force and the species buoyancy body force, respectively. The penultimate term is the Darcian linear drag and the final term is the Forchheimer quadratic drag force.

Knowing the velocity, temperature and concentration fields, it is interesting to study the local and average skin-friction, Nusselt number and Sherwood numbers are defined as follows.

Local and average skin-friction are given respectively by

$$\tau'_x = -\mu \left(\frac{\partial u}{\partial r} \right)_{r=r_0} \quad (6)$$

$$\overline{\tau}_L = -\frac{1}{L} \int_0^L \mu \left(\frac{\partial u}{\partial r} \right)_{r=r_0} dx \quad (7)$$

Local and average Nusselt number are given respectively by

$$Nu_x = \frac{-x \left(\frac{\partial T'}{\partial r} \right)_{r=r_0}}{T'_w - T'_\infty} \quad (8)$$

$$\overline{Nu}_L = - \int_0^L \left[\frac{\left(\frac{\partial T'}{\partial r} \right)_{r=r_0}}{T'_w - T'_\infty} \right] dx \quad (9)$$

Local and average Sherwood number are given respectively by

$$Sh_x = \frac{-x \left(\frac{\partial C'}{\partial r} \right)_{r=r_0}}{C'_w - C'_\infty} \quad (10)$$

$$\overline{Sh}_L = - \int_0^L \left[\frac{\left(\frac{\partial C'}{\partial r} \right)_{r=r_0}}{C'_w - C'_\infty} \right] dx \quad (11)$$

In order to write the governing equations and the boundary conditions in dimensionless form, the following non-dimensional quantities are introduced.

$$X = \frac{x\nu}{u_0 r_0^2}, \quad R = \frac{r}{r_0}, \quad t = \frac{t'\nu}{r_0^2}, \quad U = \frac{u}{u_0}, \quad V = \frac{\nu r_0}{\nu}, \quad Gr = \frac{g\beta r_0^2 (T'_w - T'_\infty)}{\nu u_0},$$

$$Gr = \frac{g\beta^* r_0^2 (C'_w - C'_\infty)}{\nu u_0}, \quad T = \frac{T' - T'_\infty}{T'_w - T'_\infty}, \quad Da = \frac{k}{r_0^2}, \quad Fs = \frac{b u_0 r_0^2}{\nu} \quad (12)$$

$$C = \frac{C' - C'_\infty}{C'_w - C'_\infty}, \quad Pr = \frac{\nu}{\alpha}, \quad Sc = \frac{\nu}{D}, \quad K_1 = \frac{K_l r_0^2}{\nu}$$

Equations (1), (2), (8) and (4) are reduced to the following non-dimensional form

$$\frac{\partial(RU)}{\partial X} + \frac{\partial(RV)}{\partial R} = 0 \quad (13)$$

$$\frac{\partial U}{\partial t} + U \frac{\partial U}{\partial X} + V \frac{\partial U}{\partial R} = GrT + GcC + \frac{1}{R} \frac{\partial}{\partial R} \left(R \frac{\partial U}{\partial R} \right) - \frac{1}{Da} U - FsU^2 \quad (14)$$

$$\frac{\partial T}{\partial t} + U \frac{\partial T}{\partial X} + V \frac{\partial T}{\partial R} = \frac{1}{Pr} \frac{1}{R} \frac{\partial}{\partial R} \left(R \frac{\partial T'}{\partial R} \right) \quad (15)$$

$$\frac{\partial C}{\partial t} + U \frac{\partial C}{\partial X} + V \frac{\partial C}{\partial R} = \frac{1}{Sc} \frac{1}{R} \frac{\partial}{\partial R} \left(R \frac{\partial C}{\partial R} \right) - K_1 C \quad (16)$$

The corresponding initial and boundary conditions are

$$t \leq 0: U = 0, V = 0, T = 0, C = 0 \quad \forall X \geq 0 \text{ and } R \geq 0$$

$$t > 0: U = 1, V = 0, T = 1, C = 1 \quad \text{at } R = 1$$

$$U = 0, V = 0, T = 0, C = 0 \quad \text{at } X = 0 \text{ and } R > 1 \quad (17)$$

$$U \rightarrow 0, T \rightarrow 0, C \rightarrow 0 \quad \text{as } R \rightarrow \infty$$

where Gr is the thermal Grashof number, Gc - solutal Grashof number, Pr - the Prandtl number, Da -Darcy number, Fr - the Forcheimmer inertial number, Sc - the Schmidt number and K_1 - non-dimensional chemical reaction parameter.

Local and average skin-friction in non-dimensional form are given by

$$\tau_x = \frac{\tau'}{\rho u_0^2} - \left(\frac{\partial U}{\partial R} \right)_{R=1} \quad (18)$$

$$\bar{\tau} = - \int_0^1 \left(\frac{\partial U}{\partial R} \right)_{R=1} dX \quad (19)$$

Local and average Nusselt number in non-dimensional form are given by

$$Nu_x = -X \left(\frac{\partial T}{\partial R} \right)_{R=1} dX \quad (20)$$

$$\bar{Nu} = - \int_0^1 \left(\frac{\partial T}{\partial R} \right)_{R=1} dX \quad (21)$$

Local and average Sherwood number in non-dimensional form are given by

$$Sh_x = -X \left(\frac{\partial C}{\partial R} \right)_{R=1} \quad (22)$$

$$\bar{Sh} = - \int_0^1 \left(\frac{\partial C}{\partial R} \right)_{R=1} dX \quad (23)$$

3. Numerical Solution

In order to solve these unsteady, non-linear coupled equations (13) to (16) under the conditions (17), an implicit finite difference scheme of Crank-Nicolson type has been employed. This method was originally developed for heat conduction problems [25]. It has been extensively developed and remains one of the most reliable procedures for solving partial differential equation systems. It is unconditionally stable. It utilizes a central differencing procedure for space and is an implicit method. The partial differential terms are converted to difference equations and the resulting algebraic problem is solved using a tri-diagonal matrix algorithm. For transient problems a trapezoidal rule is utilized and provides second-order convergence. The Crank-Nicolson Method

(CNM) scheme has been applied to a rich spectrum of complex multiphysical flows. Kafousias and Daskalakis [26] have employed the CNM to analyze the hydromagnetic mixed convection Stokes flow for air and water. Edirisinghe [27] has studied efficiently the heat transfer in solidification of ceramic-polymer injection moulds with CNFDM. Sayed-Ahmed [28] has analyzed the laminar dissipative non-Newtonian heat transfer in the entrance region of a square duct using CNFDM. Nassab [29] has obtained CNFDM solutions for the unsteady gas convection flow in a porous medium with thermal radiation effects using the Schuster-Schwartzchild two-flux model. Prasad et al [20] studied the combined transient heat and mass transfer from a vertical plate with thermal radiation effects using the CNM method. The CNM method works well with boundary-layer flows. The finite difference equations corresponding to equations (13) to (16) are discretized using CNM as follows

$$\frac{[U_{i,j}^{n+1} - U_{i-1,j}^{n+1} + U_{i,j}^n - U_{i-1,j}^n + U_{i,j-1}^{n+1} - U_{i-1,j-1}^{n+1} + U_{i,j-1}^n - U_{i-1,j-1}^n]}{4\Delta X} + \frac{[V_{i,j}^{n+1} - V_{i,j-1}^{n+1} + V_{i,j}^n - V_{i,j-1}^n]}{2\Delta R} + \frac{V_{i,j}^{n+1}}{1 + (j-1)\Delta R} = 0 \quad (24)$$

$$\begin{aligned} & \frac{[U_{i,j}^{n+1} - U_{i,j}^n]}{\Delta t} + U_{i,j}^n \frac{[U_{i,j}^{n+1} - U_{i-1,j}^{n+1} + U_{i,j}^n - U_{i-1,j}^n]}{2\Delta X} + V_{i,j}^n \frac{[U_{i,j+1}^{n+1} - U_{i,j-1}^{n+1} + U_{i,j+1}^n - U_{i,j-1}^n]}{4\Delta R} \\ & = Gr \frac{[T_{i,j}^{n+1} - T_{i,j}^n]}{\Delta t} + Gc \frac{[C_{i,j}^{n+1} + C_{i,j}^n]}{2} + \frac{[U_{i,j-1}^{n+1} - 2U_{i,j}^{n+1} + U_{i,j+1}^{n+1} - 2U_{i,j}^n + U_{i,j+1}^n]}{4(\Delta R)^2} \\ & + \frac{[U_{i,j+1}^{n+1} - U_{i,j-1}^{n+1} + U_{i,j+1}^n - U_{i,j-1}^n]}{4[1 + (j-1)\Delta R]\Delta R} - \frac{1}{Da} [U_{i,j}^{n+1} + U_{i,j}^n] - Fs U_{i,j}^n \left[\frac{U_{i,j}^{n+1} + U_{i,j}^n}{2} \right] \end{aligned} \quad (25)$$

$$\begin{aligned} & \frac{[T_{i,j}^{n+1} - T_{i,j}^n]}{\Delta t} + U_{i,j}^n \frac{[T_{i,j}^{n+1} - T_{i,j}^{n+1} + T_{i,j}^n - T_{i-1,j}^n]}{2\Delta X} + V_{i,j}^n \frac{[T_{i,j+1}^{n+1} - T_{i,j-1}^{n+1} + T_{i,j+1}^n - T_{i,j-1}^n]}{4\Delta R} \\ & = Pr \frac{[T_{i,j-1}^{n+1} - 2T_{i,j}^{n+1} + T_{i,j+1}^{n+1} + T_{i,j-1}^n - 2T_{i,j}^n + T_{i,j+1}^n]}{4(\Delta R)^2} + \frac{[T_{i,j+1}^{n+1} - T_{i,j-1}^{n+1} + T_{i,j+1}^n - T_{i,j-1}^n]}{4Pr[1 + (j-1)\Delta R]\Delta R} \end{aligned} \quad (26)$$

$$\begin{aligned} & \frac{[C_{i,j}^{n+1} - C_{i,j}^n]}{\Delta t} + U_{i,j}^n \frac{[C_{i,j}^{n+1} - C_{i-1,j}^{n+1} + C_{i,j}^n - C_{i-1,j}^n]}{2\Delta X} + V_{i,j}^n \frac{[C_{i,j+1}^{n+1} - C_{i,j-1}^{n+1} + C_{i,j+1}^n - C_{i,j-1}^n]}{4\Delta R} \\ & = \frac{1}{Sc} \frac{[C_{i,j-1}^{n+1} - 2C_{i,j}^{n+1} + C_{i,j+1}^{n+1} + C_{i,j-1}^n - 2C_{i,j}^n + C_{i,j+1}^n]}{4(\Delta R)^2} + \frac{[C_{i,j+1}^{n+1} - C_{i,j-1}^{n+1} + C_{i,j+1}^n - C_{i,j-1}^n]}{4Sc[1 + (j-1)\Delta R]\Delta R} \\ & \quad - K_1 \frac{[C_{i,j}^{n+1} + C_{i,j}^n]}{2} \end{aligned} \quad (27)$$

The region of integration is considered as a rectangle with sides $X_{\max} (=1)$ and $R_{\max} (=14)$, where

R_{\max} corresponds to $R = \infty$, which lies very well outside the momentum, energy and concentration boundary layers. The maximum of R was chosen as 14 after some preliminary investigations, so that the last two of the boundary conditions (17) are satisfied. Here, the subscript i - designates the grid point along the X - direction, j - along the R - direction and the superscript n along the t - direction. An appropriate mesh size considered for the calculation is $\Delta X = 0.05$, $\Delta R = 0.25$, and time step $\Delta t = 0.01$. During any one-time step, the coefficients $U_{i,j}^n$ and $V_{i,j}^n$ appearing in the difference equations are treated as constants. The values of U , V , T and C are known at all grid points at $t = 0$ from the initial conditions. The computations of U , V , T and C at time level $(n+1)$ using the known values at previous time level (n) are calculated as follows.

The finite difference Equation (27) at every internal nodal point on a particular i - level constitute a tri-diagonal system of equations. Such a system of equations is solved by Thomas algorithm as described in Carnahan et al. [30]. Thus, the values of C are found at every nodal point on a particular i at $(n+1)^{\text{th}}$ time level. Similarly, the values of T are calculated from the Equation (29). Using the values of C and T at $(n+1)^{\text{th}}$ time level in the Equation (26), the values of U at $(n+1)^{\text{th}}$ time level are found in a similar manner. Thus the values of C , T and U are known on a particular i - level. The values of V are calculated explicitly using the Equation (25) at every nodal point on a particular i - level at $(n+1)^{\text{th}}$ time level. This process is repeated for various i - levels. Thus, the values of C , T , U and V are known at all grid points in the rectangular region at $(n+1)^{\text{th}}$ time level. Computations are carried out till the steady state is reached. The steady state solution is assumed to have been reached, when the absolute difference between the values of U as well as temperature T and concentration C at two consecutive time steps are less than 10^{-5} at all grid points. The derivatives involved in the Equations (24) to (27) are evaluated using five-point approximation formula and the integrals are evaluated using Newton-Cotes closed integration formula. The truncation error in the finite-difference approximation is $O(\Delta t^2 + \Delta R^2 + \Delta X)$ and it tends to zero as, $\Delta X, \Delta R, \Delta t \rightarrow 0$. Hence the scheme is compatible. The finite-difference scheme is unconditionally stable as explained by Vasu et al [31]. Stability and compatibility ensures convergence.

4. Results and Discussion

Extensive computations have been performed for the effects of the controlling thermofluid and hydrodynamic parameters on dimensionless velocity (U), temperature (T) and concentration (C), and also local Skinfriction (τ_x), local Nusselt number (Nu_x), local Sherwood number (Sh_x). Only selected computations are presented in figures (2) to (20) have been reproduced here for brevity. Default values of the parameters are as follows: thermal Grashof number (Gr) = 10, species Grashof number (Gc) = 10, Prandtl number (Pr) = 0.7 (air), Darcy number (Da) = 0.1, Schmidt number (Sc) = 0.6 Forchheimer parameter (Fs) = 0.1, and Chemical parameter (K_l) = 0.5, which represents physically buoyant non-Darcian case of hydrogen diffusing in a hydromagnetic boundary layer through porous media present. All graphs therefore correspond to these values unless specifically indicated on the appropriate graph. The present analysis concerns the case of optically thick boundary layers, where the thermal boundary layer is expected to become very thick as the medium is highly absorbing.

Figure (2) to (4) illustrates the dimensionless transient velocity (U), temperature (T) and concentration (C) responses with various Forchheimer parameters (Fs) vs. R (transverse coordinate). The Forchheimer effect is a second-order nonlinear porous medium inertial resistance.

It arises also in the momentum equation (14) i.e. $-FsU^2$. Increasing F_s will evidently boost this Forchheimer drag which will decelerate the flow in the boundary layer as seen in figure (2). For increasing F_s values, the time, t , required to attain the steady state scenario is also elevated considerably. A velocity peak is again witnessed close to the cylinder surface. At some distance from the wall all profiles tend to merge and the effect of increasing F_s is greatly diminished.

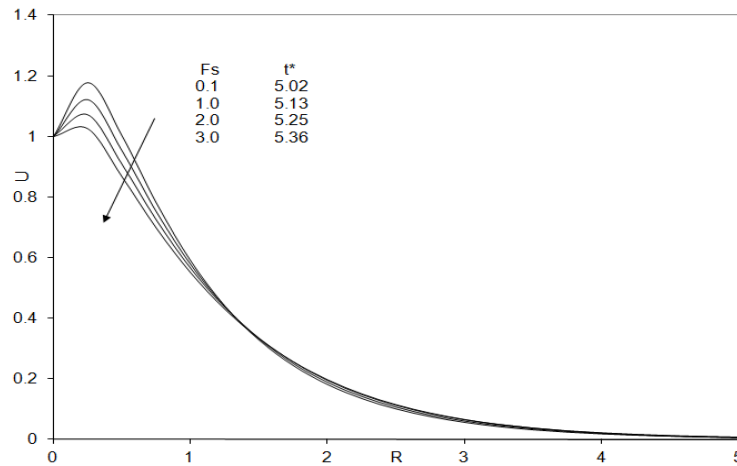


Figure 2. Steady State velocity profiles at $X=1$ for different F_s

Figure (3) shows that temperature, T is increased continuously through the boundary layer with distance from the cylinder surface, with an increase in F_s , since with flow deceleration; heat will be diffused more effectively via thermal conduction and convection. The boundary layer regime will therefore be warmed with increasing F_s and boundary layer thickness will be correspondingly increased, compared with velocity boundary layer thickness, the latter being reduced. An increase in the Forchheimer parameter (F_s), shown in Figure (4), is seen to boost the concentration distribution, in particular, in the regime, i.e. as Forchheimer drag increases, and the flow field is decelerated, contaminant is found to increase in concentration along the wall. The slower flow in the geometrical, therefore, does not have time to distribute contaminant along the wall, which accounts for higher values of C at the lower vicinity with increasing F_s values.

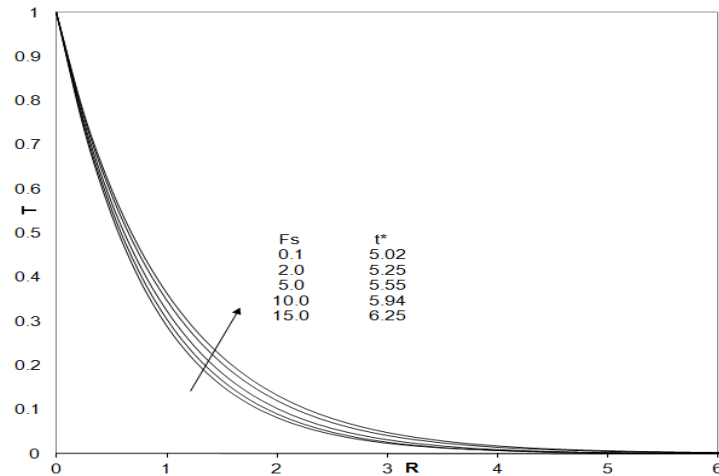
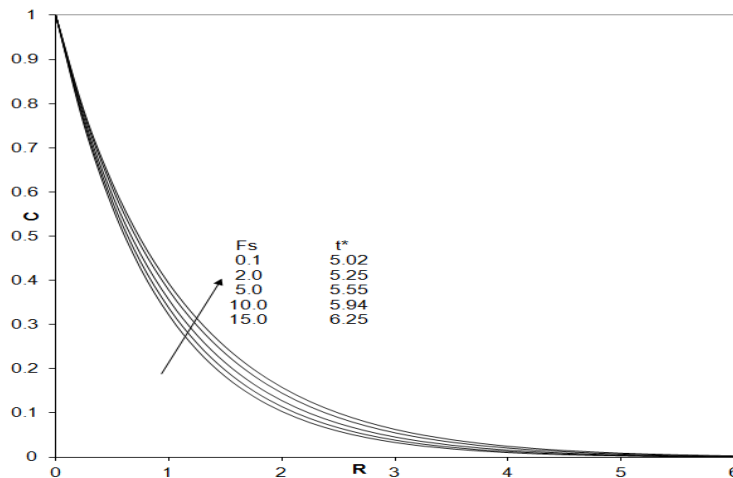
Figure 3. Steady state temperature profiles at $X=1$ for different F_s Figure 4. Steady state concentration profiles at $X=1$ for different F_s

Figure (5) and (6) depicts the effects of the bulk porous medium drag parameter, Da , on the transient velocity (U) and concentration (C) versus R profiles. This parameter, Da is directly proportional to the permeability of the regime and arises in the linear Darcian drag force term in the momentum equation (14), viz. $-\frac{U}{Da}$. As such increasing Da will serve to reduce the Darcian

impedance since progressively less fibers will be present adjacent to the cylinder in the porous regime to inhibit the flow. The boundary layer flow will therefore be accelerated and indeed this is verified in figure (5) where we observe a dramatic rise in flow velocity, U , with an increase in Da from 0.1 through 0.125, 0.15, 0.175 to 0.2. In close proximity to the cylinder surface a velocity shoot is generated; with increasing Darcy number this peak migrates slightly away from the wall into the boundary layer. Evidently lower permeability materials serve to decelerate the flow and this can be exploited in materials processing operation where the momentum transfer may require regulation.

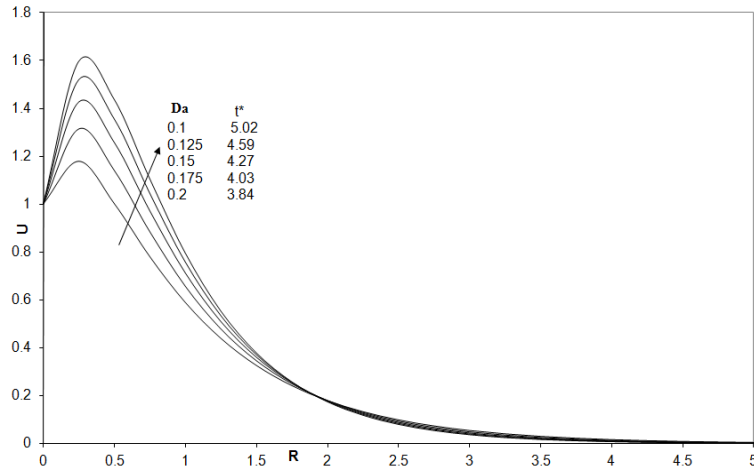


Figure 5. Steady State velocity profiles at X=1 for different Da

In figure (6) the concentration evolution (C) from the cylinder surface to the free stream with various Darcy numbers is depicted. Contrary to the velocity response, diffusion of species is stifled with increasing Darcy number i.e. concentration values decrease owing to an increase in permeability of the medium. Therefore, lower permeability media aid in the diffusion of species in the boundary layer while higher permeability regimes oppose it.

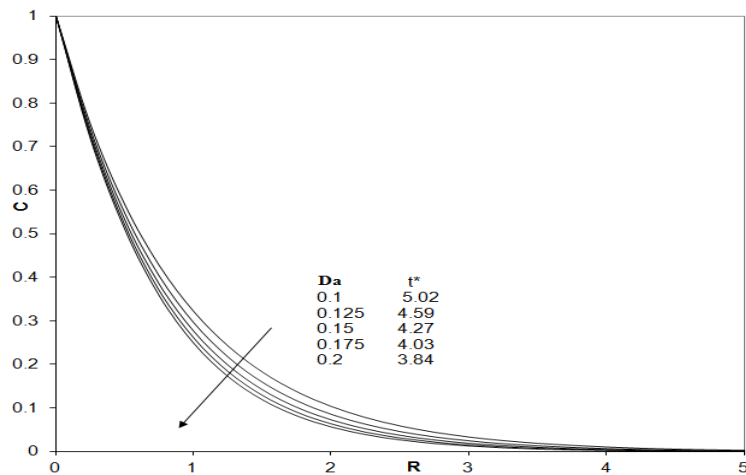


Figure 6. Steady state concentration profiles at X=1 for different Da

The effects of thermal Grashof number, Gr on velocity and temperature profiles are shown Figures. (7) and (8). Figure (7) indicates that an increase in Gr strongly boosts velocity in the boundary layer. There is rapid rise in the velocity near the wall and the peak value of the velocity at $Gr = 25$. The profiles descend smoothly towards zero although the rate of descent is greater corresponding to higher Grashof numbers. Gr defines the ratio of the thermal buoyancy force to the viscous hydrodynamic force and as expected to accelerate the flow. The temperature distributions descend smoothly from their maxima of unity at the wall ($R = 0$) to zero at the edge of the boundary layer. Thermal buoyancy therefore depresses the temperature in the medium, a result which agrees with the fundamental studies of free convection [5].

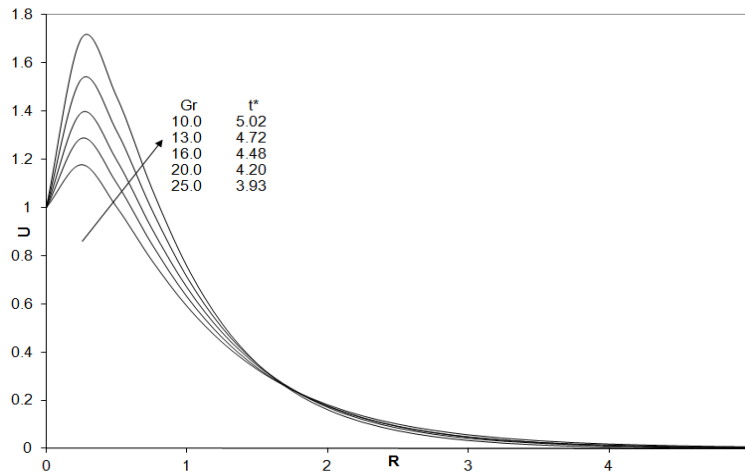


Figure 7. Steady State velocity profiles at X=1 for different Gr

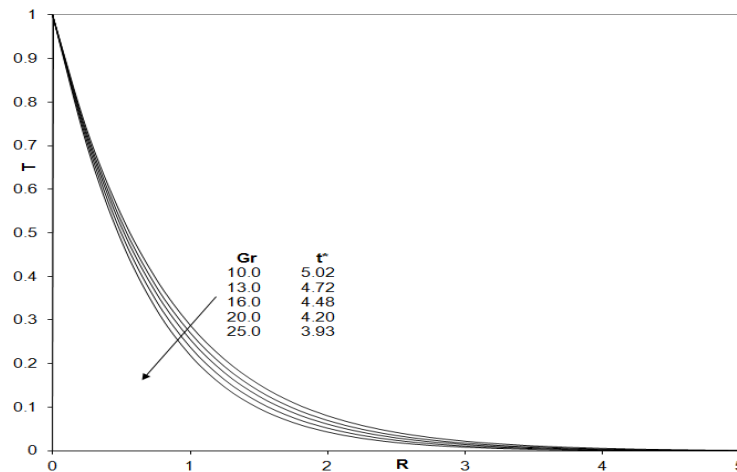


Fig 8. Steady state temperature profiles at X=1 for different Gr

The effects of species Grashof number G_c on dimensionless transient velocity (U) and concentration (C) functions are presented in Figures (9) and (10). The velocity U is observed to increase substantially with a rise in G_m from 10 to 25. Hence species Grashof number boosts the velocity of the fluid indicating that buoyancy has an accelerating effect on the flow field. Concentration, C , however undergoes a marked decrease in value with a rise in species Grashof number, as illustrated in Figure (10) The depression in concentration is maximized by larger species Grashof numbers. All profiles decay smoothly from unity at the cylinder surface to zero as $R \rightarrow \infty$.

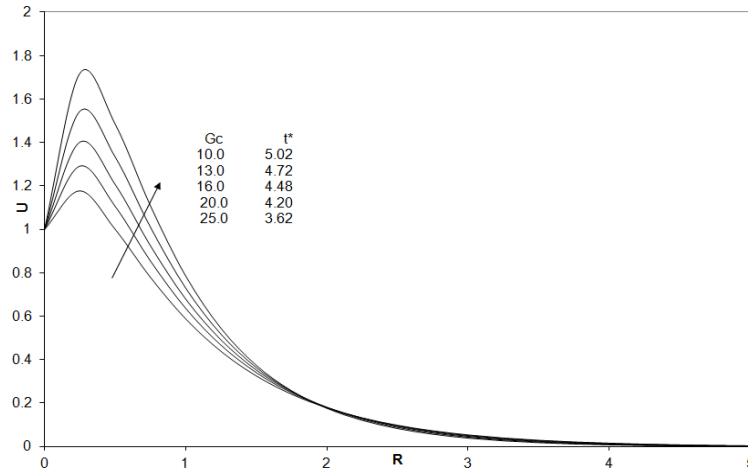


Figure 9. Steady State velocity profiles at X=1 for different Gc

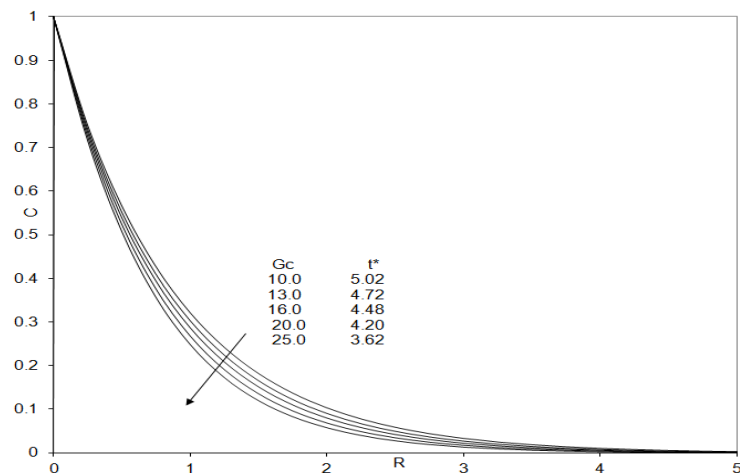


Fig 10. Steady state concentration profiles at X=1 for different Gc

The effects of Prandtl number on the dimensionless transient velocity (U) and temperature (T) profiles are depicted in Figures (11) and (12). Pr encapsulates the ratio of momentum diffusivity to thermal diffusivity. Larger Pr values imply a thinner thermal boundary layer thickness and more uniform temperature distributions across the boundary layer. With increasing Pr values, the time, t , required to attain the steady state scenario is also elevated considerably. For $Pr=1$, the momentum and thermal boundary layer thicknesses, as described by Schlichting [32], are approximately of equal extent. Smaller Pr fluids have higher thermal conductivities so that heat can diffuse away from the surface of the cylinder than for higher Pr fluids. We therefore expect that an increase in Pr the thermal boundary layer will be decreased in thickness and there will be corresponding uniformity of temperature distributions across the boundary layer. The computations show that the velocity is therefore reduced as Pr rises from 0.71, through 1.0, 2.0 and 4.0, since the fluid is increasingly viscous as Pr rises. Hence the fluid is decelerated with a rise in Pr . Figure (12) indicates that a rise in Pr substantially reduces the temperature, in the fluid saturated porous regime. For all cases, velocity and temperature decay smoothly to zero as $R \rightarrow \infty$, i.e. in the free stream.

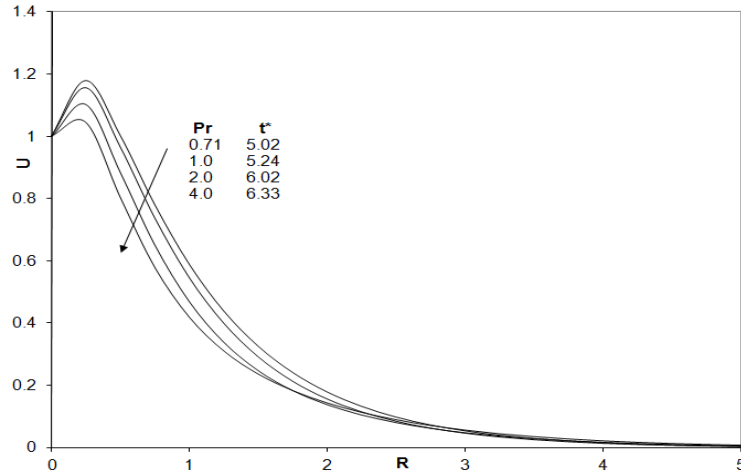


Figure 11. Steady State velocity profiles at X=1 for different Pr

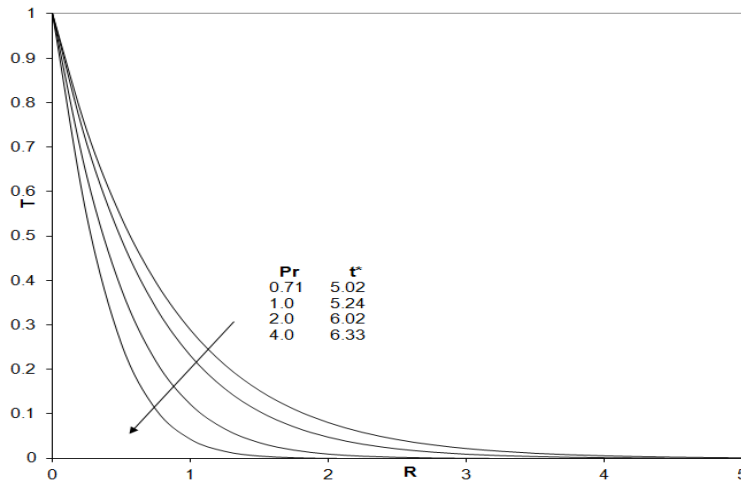


Figure 12. Steady state temperature profiles at X=1 for different Pr

The effect of Sc on dimensionless concentration is shown Figure (13). Sc , i.e. Schmidt number, embodies the ratio of the momentum to mass diffusivity. Sc therefore quantifies the relative effectiveness of momentum and mass transport by diffusion in the hydrodynamic and concentration boundary layers. We have presented the computations for $Pr = 0.7$. In all profiles for different Sc values, $Pr \neq Sc$. The thermal and species diffusion regimes are of different extents. As Sc increases, Figure (13) shows that concentration (C) values are strongly decreased, as larger values of Sc correspond to a decrease in the chemical molecular diffusivity i.e. less diffusion therefore takes place by mass transport. The time required to reach the steady state increases with the increase in Sc . The dimensionless concentration profiles all decay from a maximum concentration of 1 at $R=0$ (the wall boundary condition) to zero in the free stream.

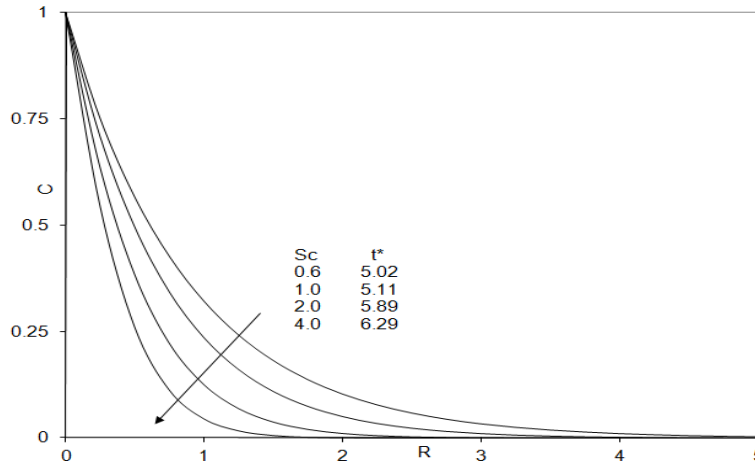


Figure 13. Steady state concentration profiles at X=1 for different Sc

Figures (14) to (16) display the influence of chemical reaction parameter (K_1) on the transient velocity (U), temperature (T) and concentration (C) profiles and time, t. The effect of velocity for different chemical reaction parameter ($K_1 = 0.5, 1.0, 2.0, 4.0$), $Gr = Gc = 5$, $Fs = Da = 0.1$, $Pr = 0.71$ and $Sc = 0.6$ are shown in Figure (14). It is observed that the velocity increases with decreasing chemical reaction parameter. It is seen that as an increase of chemical reaction parameter leads to increase temperature profiles. Figure (16), represents the effect of concentration profiles for different chemical reaction parameter K_1 . The effects of chemical reaction parameter play an important role in concentration field. There is a fall in concentration due to increasing the values of the chemical reaction parameter. However, with progressive of time the concentration is found to be decreased in the boundary layer regime.

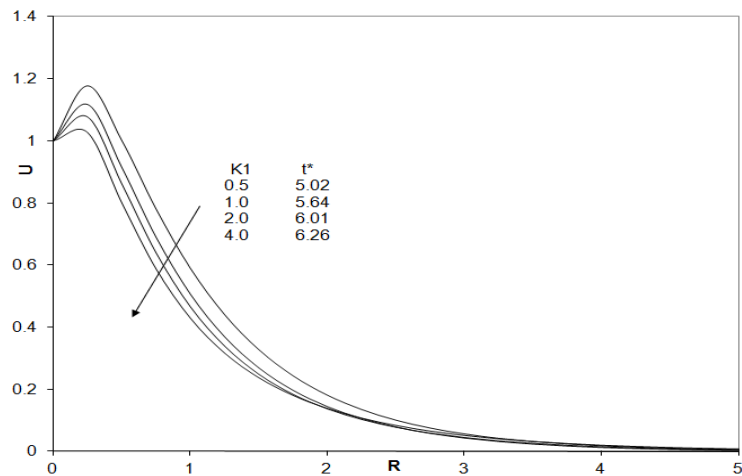


Figure 14. Steady state velocity profiles at X=1 for different K1

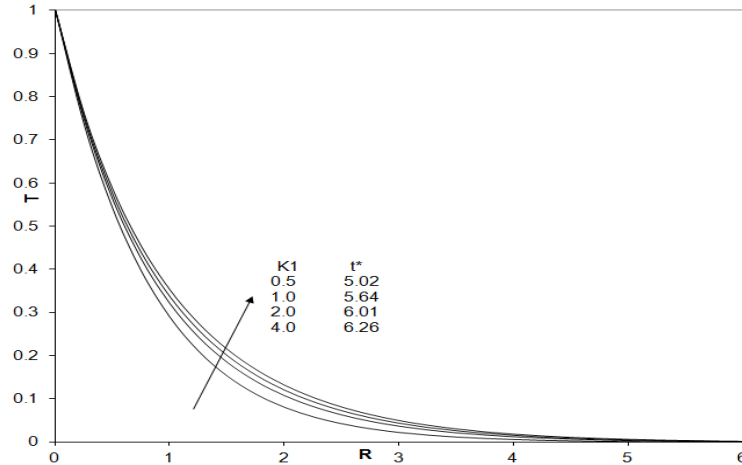


Figure 15. Steady state temperature profiles at $X=1$ for different K_1

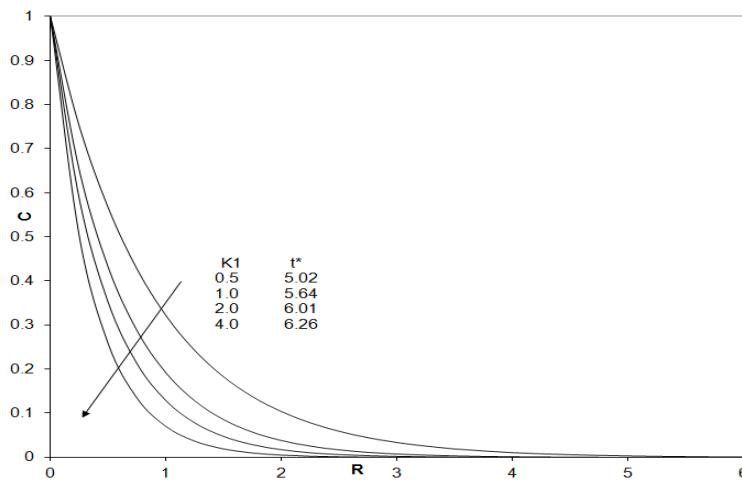


Figure 16. Steady state concentration profiles at $X=1$ for different K_1

Knowing the velocity and temperature field, it is customary to study the skin-friction, the Nusselt number and Sherwood number. The derivatives involved in the equations (18) to (23) are evaluated using five-point approximation formula and then the integrals are evaluated using Newton-Cotes closed integration formula.

The Local values of the skin-friction, Nusselt number and Sherwood number for fixed parameters $Gr = Gc = 10$, $Pr = 0.71$, $Da = 0.1$, $Fs = 0.1$, $K_1 = 0.5$ and $Sc = 0.6$ are plotted in Figures (17) to (20) respectively. Local skin-friction values are evaluated from equation (28) and plotted in Figure (17) as a function of the axial coordinate. The local wall shear stress increases with increasing chemical reaction parameter. The value of the skin-friction becomes negative, which implies that after some time there occurs a reverse type of flow near the moving cylinder. Physically this is also true as the motion of the fluid is due to cylinder moving in the vertical direction against the gravitational field. The rate of heat transfer increases with decreasing values of the chemical reaction parameter. The Local Nusselt number for different values of the both Forchheimer parameter, Darcy number and chemical reaction parameter is shown in Figure (18). The trend shows that the Local Nusselt number decreases with increase both chemical reaction parameter and Forchheimer parameter while Darcy number decreases. The Local Sherwood numbers for

different values of the chemical reaction parameter and Forchheimer parameter are shown in Figure (19) and (20). The trend shows that the rate of concentration decreases the presence of chemical reaction and Forchheimer parameter than their absence.

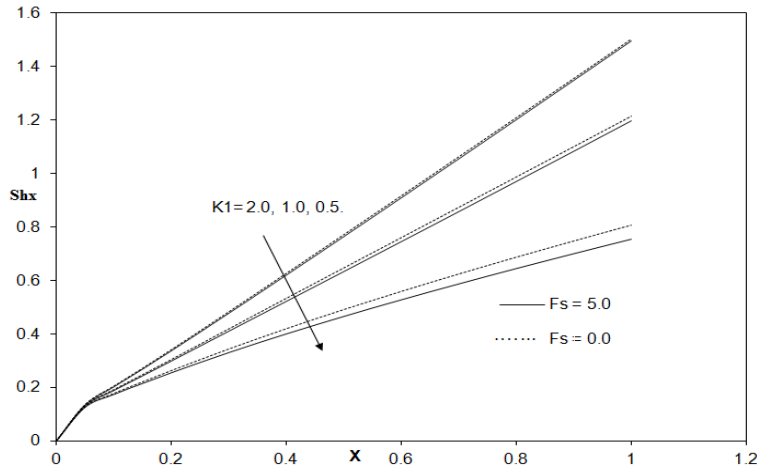


Figure 17. Local Sherwood number distribution for several of K_1 and F_s .

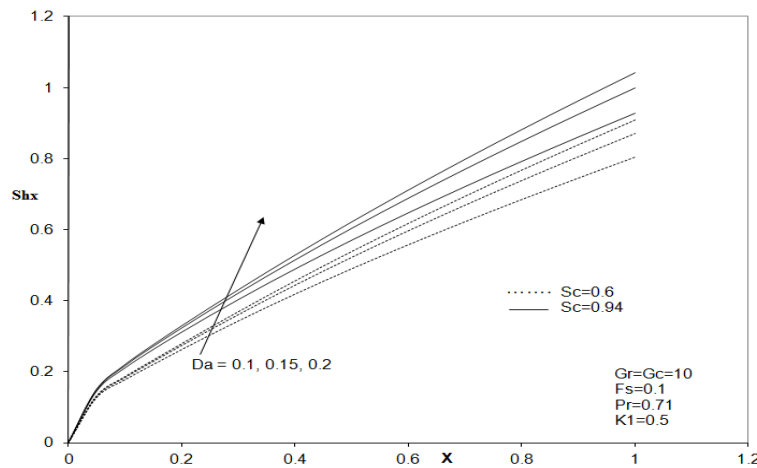


Figure 18. Local Sherwood number distribution for several of Da and Sc .

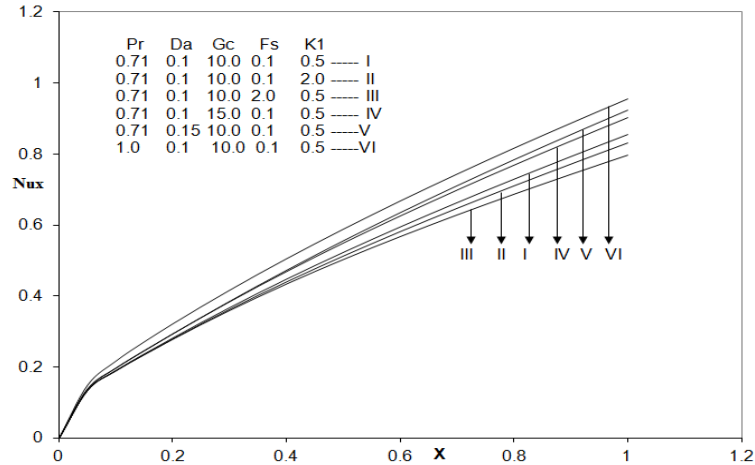


Figure 19. Local Nusselt number distributions

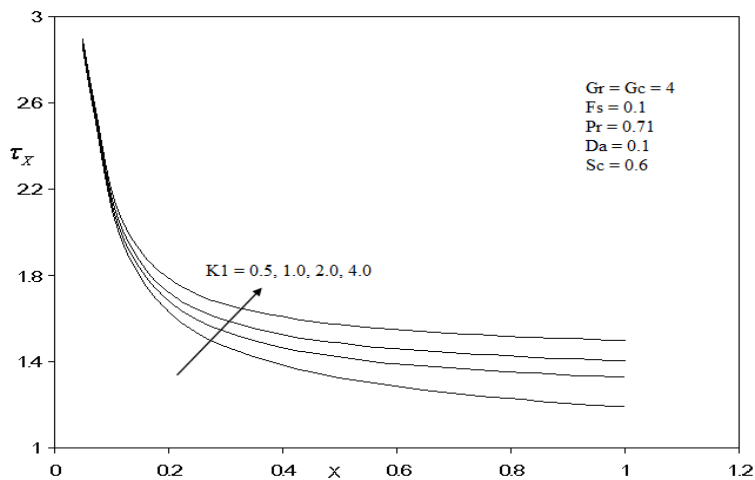


Figure 20. Local Skin friction distributions for various K1

5. Conclusions

A detailed mathematical study for the chemically-reactive unsteady, free convection heat and mass transfer boundary layer flow along a vertical cylinder embedded in a non-Darcy porous medium, has been conducted. Computational solutions to the dimensionless conservation equations have been obtained using the implicit finite-difference scheme of Crank-Nicolson type. It has been shown that an increasing Darcy number is seen to accelerate the flow but decreases concentration values in the regime. Increasing Forchheimer inertial drag parameter (F_s) reduces velocities but elevates temperatures and concentration values. The velocity as well as concentration decreases with increasing the chemical reaction parameter (K_1). Local Sherwood number is enhanced with a rise in Schmidt number Sc and Da , decreases with increasing F_s and K_1 . i.e. greater rates of concentration transfer of contaminant occur for lower porous resistance effects. The present numerical code based on the robust, implicit finite-difference scheme of Crank-Nicolson type has been shown to produce excellent results. Very good correlation between the present computations and the trends of other previous studies has been identified. Further investigations will consider transient effects and employ the Keller-box method to consider more complex chemical engineering phenomena including electrophoretic deposition, nanofluids and thermophoresis.

Acknowledgment

The authors are grateful to Motilal Nehru National Institute of Technology Allahabad for providing academic facilities to carry out this research work.

References

- [1] E.M. Sparrow and J.L. Gregg, The laminar free convection heat transfer from the outer surface of a vertical cylinder, *Trans. ASME*, vol. 78, pp. 1823, 1956.
- [2] W.J. Minkowycz and E.M. Sparrow, Local Nonsimilarity Solutions for Natural Convection on a Vertical Cylinder, *J. Heat Transfer*, vol. 96, pp. 178-183, 1974.
- [3] T. Fujii and H. Uehara, Laminar natural-convection heat transfer from the outer surface of a vertical cylinder, *Int. J. Heat Mass Transfer*, vol. 13, pp. 607–615, 1970.
- [4] H.R. Lee, T.S. Chen and B.F. Armaly, Natural convection along vertical cylinders with variable surface temperature, *J. Heat Transfer*, vol.110, pp. 103-108, 1988.
- [5] H.P. Rani, Transient natural convection along a vertical cylinder with variable surface temperature and mass diffusion, *Heat and Mass Trans.*, vol. 40, pp. 67-73, 2003.
- [6] P. Ganesan and P. Loganathan, Radiation and mass transfer effects on flow of an incompressible viscous fluid past a moving vertical cylinder, *Int. Journal of Heat and Mass Trans.*, vol. 45, pp. 4281-4288, 2002.
- [7] U.N. Das, R.K. Deka and V.M. Soundalgekar, Effects of mass transfer on flow past an impulsively started infinite vertical plate with chemical reaction, *The Bulletin of GUMA*, vol. 5, pp.13-20, 1999.
- [8] A.Y. Ghaly and M.A. Seddeek, Chebyshev finite difference method for the effects of chemical reaction, heat and mass transfer on laminar flow along a semi infinite horizontal plate with temperature dependent viscosity, *Chaos Solitons & Fractals*, vol. 19(1), pp.61-70, 2004.
- [9] R. Muthucumaraswamy and P. Ganesan, First-order chemical reaction on flow past an impulsively started vertical plate with uniform heat and mass flux, *Acta Mechanica*, vol. 147, issue 1-4, pp. 45-57, 2001.
- [10] P. Ganesan and P. Loganathan, Heat and mass transfer flux effects on a moving vertical cylinder with chemically reactive species diffusion, *J. Engineering Physics and Thermodynamics*, vol. 75 Issue 4, pp. 899-909, 2002.
- [11] D.B. Ingham and I. Pop, *Transport Phenomena in Porous Media*. Elsevier Science, Oxford, 1998.
- [12] D.A. Nield, A. Bejan, *Convection in Porous Media*, Springer, New York, 2013.
- [13] P. Singh, J.K. Misra and K.A. Narayan, Free convection along a vertical wall in a porous medium with periodic permeability variation, *Int. J. Numer. Anal. Methods Geomech.*, vol.13(4), pp. 443–450, 1989.
- [14] H.R. Thomas, and C.L.W. Li, Modelling transient heat and moisture transfer in unsaturated soil using a parallel computing approach, *Int. J. Numer. Anal. Methods Geomech*. Vol. 19, No. 5, pp. 345–366, 1989.

- [15] A. Dybbs, R.V. Edwards, A new look at porous media fluid mechanics: Darcy to turbulent, In: B. Corapcioglu (eds.), *Fundamentals of Transport Phenomena in Porous Media*, NATO Applied Science Series E, pp 199–256, The Netherlands, 1984.
- [16] M. Kumari, H.S. Takhar and G. Nath, Non-Darcy double-diffusive mixed convection from heated vertical and horizontal plates in saturated porous media, *Thermo Fluid Dynamics, Wärme-und Stoffübertragung*, vol. 23, pp. 267–273, 1988.
- [17] H.S. Takhar, O.A. Bég, Non-Darcy convective boundary layer flow past a semi-infinite vertical plate in saturated porous media, *Heat Mass Transf. J.*, vol. 32, pp. 33–44, 1996.
- [18] O.A. Bég, J. Zueco, H.S. Takhar and A. Sajid, Transient Couette flow in a rotating non-Darcian porous medium parallel-plate configuration - network simulation method solutions, *Acta Mech.* vol. 202, pp. 181-204, 2008.
- [19] V.R. Prasad, B. Vasu, O.A. Bég, and R. Parshad, Unsteady Free Convection Heat and Mass Transfer in A Walters-B Viscoelastic Flow Past a Semi-infinite Vertical Plate: A Numerical Study, *Thermal Science*, Vol.15, Suppl. 2, S291-S305, 2011.
- [20] V.R. Prasad, N.B. Reddy and R. Muthucumaraswamy, Radiation and mass transfer effects on two-dimensional flow past an impulsively started infinite vertical plate, *Int. J. Thermal Sciences*, vol. 46(12), pp.1251-1258, 2007.
- [21] C. Israel-Cookey, E. Amos and C. Nwaigwe, MHD oscillatory Couette flow of a radiating viscous fluid in a porous medium with periodic wall temperature, *Am. J. Sci. Ind. Res.*, vol. 1, pp.326-331, 2010.
- [22] C. Huang, Lateral mass flux and thermal radiation on natural convection heat and mass transfer from a vertical flat plate in porous media considering Soret/Dufour effects, *Journal of King Saud University – Science*, Article in press, (2016).
- [23] P.K. Sharma and M. Dutt, MHD oscillatory free convection flow past parallel plates with periodic temperature and concentration, *Univ. J. Appl. Math.*, vol. 2(7), pp. 264-75, 2014.
- [24] C.N. Muli and J.K. Kwanza, Cross-Diffusion effect on mixed convective fluid flow through horizontal annulus, *Math. Theory and Modelling*, vol.4(5), pp. 31-49, 2014.
- [25] J. Crank and P. Nicolson, A practical method for numerical evaluation of solutions of partial differential equations of the heat conduction type, *Proc. Camb. Phil. Society*, vol. 43, pp. 50-67, 1947.
- [26] N.G. Kafousias and J. Daskalakis, Numerical solution of MHD free-convection flow in the Stokes problem by the Crank-Nicolson method, *Astrophysics and Space Science*, vol. 106(2), pp.381-389, 1984.
- [27] M.J. Edirisinghe, “Computer simulating solidification of ceramic injection moulding formulations, *J. Materials Science Letters*, vol. 7, No. 5, pp.509-510, 1988.
- [28] M.E. Sayed-Ahmed, Laminar heat transfer for thermally developing flow of a Herschel-Bulkley fluid in a square duct, *Int. Comm. Heat Mass Transfer*, vol. 27(7), pp.1013-1024, 2000.
- [29] A.S.G. Nassab, Transient heat transfer characteristics of an energy recovery system using a porous medium, *IMEchE J. Power and Energy*, vol. 216(5), pp.387-394, 2002.

- [30] B. Carnahan, H.A. Luther and J.O. Wilkes, Applied Numerical Methods, John Wiley and Sons, New York, 1969.
- [31] B. Vasu, V.R. Prasad and B. Reddy, Radiation and Mass Transfer Effects on Transient Free Convection Flow of a Dissipative Fluid past Semi-Infinite Vertical Plate with Uniform Heat and Mass Flux, Journal of Applied Fluid Mechanics, Vol 4(1), pp. 15-26, 2011.
- [32] H. Schlichting, Boundary Layer Theory, Mac Graw Hill, New York, 7th Edition, 1979.

Biographical information

Buddakkagari Vasu was born in Tekumanda, Chittoor District, Andhra Pradesh, India in May, 1981. He obtained his Masters degree in Mathematics (2003) and Doctoral degree in Fluid Dynamics (2011), thesis title: ‘Thermo-Diffusion and Diffusion-Thermo effects on Free Convective Boundary Layer Flows’ under the supervision of Prof N. Bhaskar Reddy from Sri Venkateswara University, Tirupati. He then worked as Assistant Professor in the Department of Mathematics, Madanapalle Institute of Technology and Science, India for seven years (2005- 2012). Since October 2012 he is working as Assistant Professor in the Department of Mathematics, Motilal Nehru National Institute of Technology Allahabad, India. His primary research interests are directed towards Fluid Dynamics, Heat and Mass Transfer, Nanofluids and Bio-fluids Flow Modelling, Newtonian and non-Newtonian Boundary Layer Flows. During my teaching and research, he has been developed some numerical codes for implicit Keller-box numerical programs to nonlinear fluid dynamics and thermal sciences problems. Apart from his research skills, he has authored or co-authored over twenty seven journal papers in good impact factor international journals and 3 books/book chapter. In addition to his research skills, he has developed presentation, team working and organization skills. He has been awarded UGC Research



Award for 2014-16 by University Grants Commission, India.

Rama S. R. Gorla is presently working as Visiting Professor in the Department of Mechanical & Civil Engineering at Purdue University Northwest. Prior to this, he was Fenn Distinguished Research Professor in the Department of Mechanical Engineering at Cleveland State University. He received the Ph.D. degree in Mechanical Engineering from the University of Toledo in 1972. His primary research areas are combustion, heat transfer and fluid dynamics. He was involved in the testing and development of a three-dimensional Navier Stokes Computational Code for Wright Patterson Air Force Base. He worked as a turbomachinery design engineer at Teledyne Continental Motors Turbine Engines (TCM-TE) in Toledo, Ohio and as a design engineer of the aerothermodynamics of rotating machinery at Chrysler Corporation in Highland Park, Michigan. He completed a research program funded by NASA Lewis Research Center in Turbine Heat Transfer. Dr. Gorla has published over 550 technical papers in refereed journals and contributed several book chapters in Encyclopedia of Fluid Mechanics. NASA, AFOSR and local industry have sponsored his research. He co-authored text books on Advanced Differential Equations published by Studera Press in 2016 and Turbomachinery published by Marcel &



Dekker Company in 2003. He is the recipient of two Distinguished Faculty awards from Cleveland State University, the first for research in 1999 and the second for teaching in 2004. He was given the Teaching Excellence Award from the Northeast Ohio Council on Higher Education in 2004. He received the Distinguished Technical Educator Award from the Cleveland Technical Societies Council in May 2006. He serves on the editorial board of several journals.

V. R. Prasad was born in Madanapalle, Chittoor District, Andhra Pradesh, India in July, 1968. He obtained a Distinction Class Masters of Sciences, degree in Mathematics (1994) from Osmania University, Hyderabad and a PhD in Radiation and Mass Transfer Effects on convective flow past a vertical plate (2003), both from Sri Venkateswara University, Tirupati. He then worked as lecturer in the Department of Mathematics, Besant Theosophical College, Madanapalle, India for seven years (1994-2001). From May 2001 to April 2007, he was an Assistant Professor for six years in the Department of Mathematics, in Madanapalle Institute of Technology and Science. Later from May 2007 to April 2009 worked as Associate Professor, in the Department of Mathematics, Madanapalle Institute of Technology and Science, Madanapalle, India. Form May 2009 to till date he is working as Professor in the Department of Mathematics, Madanapalle Institute of Technology and Science, Madanapalle, India. He has authored Radiation effects on Convective Flow Past a Vertical Plate: Radiation and Mass Transfer Effects on Convective Flow Past a Vertical Plate, (Lambert, Germany, 2010), Thermo-Diffusion and Diffusion-Thermo Effects on Boundary Layer Flows (Lambert, Germany, 2011) and Walters_B Viscoelastic flow Past a Vertical Plate: Numerical Study of Unsteady



Free Convective Heat and Mass Transfer in a Walters_B Viscoelastic Flow Past a Vertical Plate (Lambert, Germany, 2012). He has published in excess of 50 journal articles. His research has also been presented at over 13 conferences. He is currently engaged in simulating different non-Newtonian fluids from curved bodies.

O. A. Beg was born in Dewsbury, Yorkshire, England in September, 1969. He obtained a First Class BEng (Hons) degree in Engineering (1992) and a PhD in Computational Magnetohydrodynamics (1996), both from the University of Manchester. He then worked in industrial consultancy for five years where he was involved with aero-structural analysis/dynamics, fire dynamics modeling and geomechanics. He attended the First MIT Conference in Computational Fluid and Solid Mechanics. He was Course Director of the BSc (Hons) in Fire Safety Engineering Sciences at Leeds Metropolitan University for five years, where he also taught engineering mathematics, fire dynamics, explosion sciences, thermofluids and acoustics. He then taught aerodynamics at BAE Systems, Riyadh, Arabia and was engaged in researching hypersonic and electromagnetic propulsion. He was subsequently Director of the MEng (Hons) degree in Aerospace Engineering at Sheffield Hallam University. Since March 2016 he has been working in coating fluid mechanics, corrosion modeling, bio-propulsion and nanosystems at the University of Salford. He is also actively engaged in supervising aerospace research dissertations in aerodynamics, bio-inspiration, hybrid propulsion and nanomaterials. He has been an Associate Editor of the Journal of Mechanics in Medicine and Biology since 2010. He has published over 340 journal papers and five books in magnetohydrodynamics, micropolar fluid



dynamics and the history of engineering science. He recently co-edited the book “Modeling and Simulation in Engineering Sciences”, published by Intech Press. His

heroes in science are A.C. Eringen, pioneer in engineering sciences and L.D. Landau, pioneer in superfluidity and superconductivity.